COMPUTATIONAL STUDY OF ELECTRIC FIELD TREATMENT AT BONE-NEIGHBORING TUMORS

Pedro José Teixeira Pagano
Jéssica Rodrigues da Silva
Daniella de Lourdes Luna Santana de Andrade
Guilherme Brasil Pintarelli
Jennifer Farias Rodrigues
Daniela Ota Hisayasu Suzuki
Biomedical Engineering Institute, Federal University of Santa Catarina, Florianópolis - Brazil
pedroo.pagano@gmail.com, sracissej@gmail.com, dani.dllsa@gmail.com, guilherme.b.pintarelli@gmail.com,
posgraduacaoiebufscjennifer@gmail.com, daniela@ppgeel.ufsc.br

Abstract. Electrochemotherapy success is directly related to tumor electric field coverage, and the coverage failure may result in tumor recurrence and pain. The electric field may diffract during nodule treatment due to surrounding dielectrics and non-linear dynamic response to electroporation. Computational models are used to study this complex process and optimize the treatment. Bone is characterized as a low electric conductivity material, and if located near tumor regions, it may affect the electric field distribution. This paper aims to assess the electric field distribution in cancer-infected tissue near bones. We calculated the electric field distribution using computational simulations (COMSOL Multiphysics). Our case study was a dogs' nasal cavity tumor surrounded by bone (semi ellipsoid). We investigated whether the voltage pulses would meet electrochemotherapy electric field requirements. This is, minimizing the lack of an insufficient electrical field, the so-called indentation. We studied a range of 282.4 to 529.5 V applied to a recently ECT electrode apparatus. We also studied if a conductive gel could enhance the electrical field distribution. Results showed that high electric field application does not solve the indentation problem. The electric field indentation was detected from approximately 3 mm electrode-bone proximity region at the lowest electric fields and increased to 5 mm at 150 kV/m. The electric field indentation mostly occurred due to the bone insulator behavior. The use of the conductive gel also led to indentation. The tumor volume coverage is reduced when compared with simulations without gel, thus it is not recommended for use in this situation.

Keywords: electromechanical properties of tissues, cancer treatment, ESOPE, complex geometry problems

1. INTRODUCTION

Electroporation (EP) is a cell permeability-increasing phenomenon that occurs when pulsed electric fields (PEF) are applied to the plasma membrane (Prausnitz *et al* 1993). The increase in permeability, *i.e.,* conductivity, is explained by the opening of pores near the cell poles. The EP can be modulated according to the electric field (EF) magnitude and pulse length. If the pores reseal after application, EP is reversible. If the pores cannot close or the cell is damaged, EP is irreversible (Teissié and Rols 1993, Suzuki *et al* 2011). Long pulse duration and high amplitude are related to the Joule effect and electrolysis, not EP; in this case, the exceeding electric field conducts the cell to death by thermal and pH damage (Rubinsky 2007).

The EP techniques are widely employed in food processing and conservation (Heinz *et al* 2001), extraction of macromolecules (Kotnik *et al* 2015) and in medicine as a cancer treatment called Electrochemotherapy (ECT). The ECT uses reversible EP to catalyze the effects of chemotherapy drugs in tissues (Suzuki *et al* 2018). The European Standard Operating Procedures of ECT (ESOPE) was released in 2006 (Mir *et al* 2006) and updated in 2018 (Gehl *et al* 2018). Those are guidelines for ECT treatment, *i.e.,* electrical specifications for electrodes and pulses protocols and clinical methods.

The ECT is successful if the applied electric field manages to cover the entire tumor mass. In clinical and veterinary procedures, the treatment feedback is the decrease of the tumor volume, which may take weeks. Thus, ECT procedures require precise treatment planning. In this sense, mathematical models are an essential tool for predicting physiologic and chemical changes in biological tissues (Miklavčič 2017). These models can predict tissue volume coverage and the suitable electrode configuration. The literature recommends using static numerical models of electric field-dependent conductivity (*e.g.* based on Finite Element Method or Finite Difference Method) to explain the non-linear increase of the conductivity and field distribution due to pore formation (Suzuki *et al* 2018, Tamzali *et al* 2012). Yet, some deep-seated tumors are known to be challenging for ECT. Deep-seated tumors may have anatomical complexity, such as diverse tissues in the tumor neighborhood. In addition, the conductivity and the EP model depend on the tissue's characteristics, such as vascularization and oxygen concentration (Sieni *et al* 2020).

In pre-treatment, one must consider that the tumor neighboring structures can also interfere with the dielectric response to ECT. Bone tissue is characterized as a low electric conductivity material and its presence could lead to electric field coverage issues depending on how close it is to the tumors (Suzuki *et al* 2017). This paper aims to assess the electric field distribution in a dog's intranasal cavity tumor case study using computer modeling. The tumor region is surrounded by irregular bone structure. We used a recently developed ECT single needle electrode apparatus to reach the tumor area.

2. METHODS

This study analyzed the *in silico* EF distribution of a geometry similar to a dog intranasal region and a single needle electrode apparatus (Maglietti *et al* 2017). The geometry is shown in Fig. 1. The 3D geometry consists of a nylon insulator cylinder with 19 mm of height and 5 mm of diameter, and two stainless steel plate electrodes with 0.1 mm width and 3.5 mm separation gap (from arc length distance reference) inserted in a semi ellipsoid tumor geometry (20 mm height, and 28 mm maximum diameter), and surrounded by bone (22 mm height, and 36 mm maximum diameter). The semi ellipsoid geometry is a geometry approximation to the ends of the nasal cavity of a dog infected with tumor tissue (Kluthcovsky *et al* 2021).

The computational model was performed with FEM software COMSOL Multiphysics v.5.1 (COMSOL Inc., Stockholm, Sweden) running on a cluster server (Intel Xeon Gold 6126 @ 2.60 GHz, 20 cores, 300 GB RAM) with Ubuntu Linux (x64, Canonical Ltd. London, United Kingdom) operating system. The finer-grained mesh was automatically generated by the software, resulting in approximately 733k tetrahedral elements. COMSOL solves the equation of continuity for a steady-state regime shown in Eq. (1).

$$-\nabla \cdot (\sigma \cdot \nabla V) = 0 \qquad (1)$$

where σ is the tissue electrical conductivity (S/m), and V is the electric potential (V). The boundary conditions were all insulating on the external surfaces (Neumann's boundary condition). The contact between electrode and tissue was modelled as Dirichlet's boundary condition. EP changes the tissue properties and also its electrical conductivity. Equation (2) describes the tissue conductivity under exposure to PEF as used by Sel *et al*., (Šel *et al* 2005).

$$\sigma(E) = \sigma_0 + \frac{\sigma_{MAX} - \sigma_0}{1 + D \cdot e^{-\frac{E-A}{B}}} \qquad (2)$$

$$A = \frac{E_{IRE} + E_{RE}}{2}, \qquad B = \frac{E_{IRE} - E_{RE}}{C}, \qquad C = 8, \qquad D = 10$$

where σ is the electrical conductivity (S/m), and E is the applied electric field (V/m). The reversible and irreversible EP thresholds are given by E_{RE} and E_{IRE}, respectively. The constants *C* and *D* are the sigmoid function parameters. The electrical conductivity of bone tissue was considered constant and equal to 0.013 S/m (Gabriel *et al* 2000). The initial conductivity of tumor tissue is $\sigma_0 = 0.30$ S/m, and the maximum conductivity with PEF is $\sigma_{MAX} = 0.75$ S/m, and $E_{IRE} = 80$ kV/m, $E_{RE} = 40$ kV/m (Šel *et al* 2005).

We investigated whether increasing the applied voltage would eliminate the EF coverage issue in tissue caused by bone proximity, classified as indentation. In Fig. 1(a), *p* represents the distance between the electrode lateral surface and bone. At the superior region of the electrode, it has the maximum distance (*p* = 11.5 mm) and decreases reaching the minimum distance (*p* = 1.89 mm) at the deepest electrode portion of the geometry. Indentation is also dependent on the EF strength. We applied the following voltages: 282.4, 317.7, 353, 388.3, 423.6, 458.9, 494.2 and 529.5 V (80 to 150 kV/m, 10 kV/m steps). We analyzed the geometry cut planes perpendicular to electrode insertion to assess p and the electric currents for each applied voltage.

Following, we added a 1.5 mm layer of a conductive gel (0.1 S/m) around the last 5 mm depth of the electrode, as shown in Fig. 1(b). We analyzed the electric field distribution and tested if it could set a lower voltage to meet the ECT criteria (*i.e.*, minimize the indentation in the tumor portion caused by bone presence).
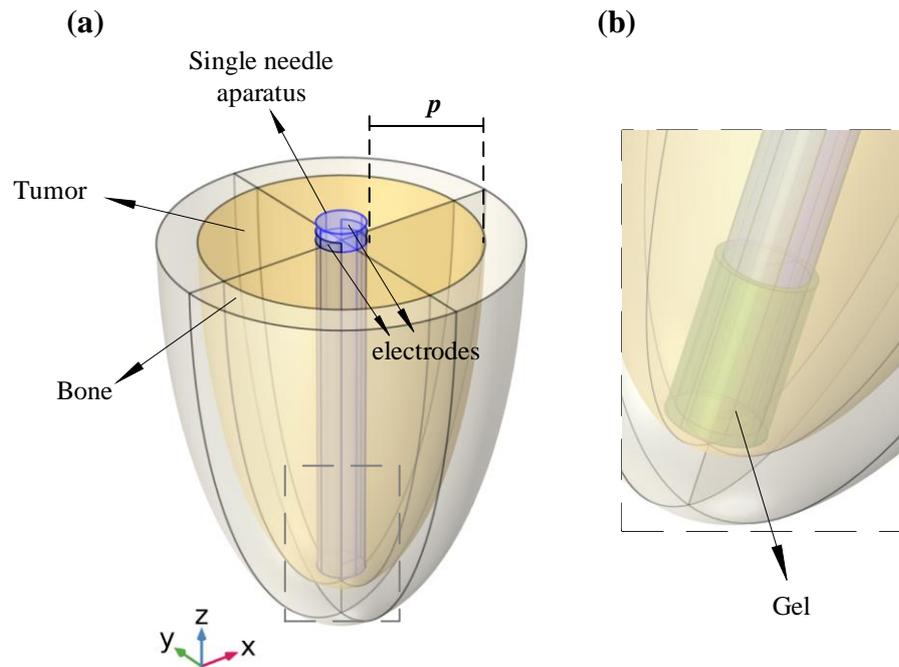
(a) **(b)**

Figure 1. The geometry of the case study. (a) Tumor mass (yellow) surrounded by bone tissue (translucent white) represents a dog's intranasal cavity. The needle aparatus (blue) is inserted into the tumor. (b) The implemented layer of the 0.1 S/m conductive gel at the last 5 mm depth of the electrode .

3. RESULTS

Table 1 shows the measured electric currents and the electrode-bone distance p for each applied EF, and Fig. 2 shows the EF distribution in the top and bottom cut planes of tumor for 80, 110 and 150 kV/m without and with the 0.1 S/m conductivity gel. At the least bone proximity (top region), the EF is less narrowed and without indentation . Bottom slices without gel show that the bone presence interferes in the field distribution, resulting in indentation. Bottom cut planes with gel insertion resulted in less EF volumes and consequently less EP coverage. Still, EF indentations are detected from 423.6 V application (120 kV/m) using the gel.

Table 1. *In silico* results of electric currents and electrode-bone distance p for electric field indentation.

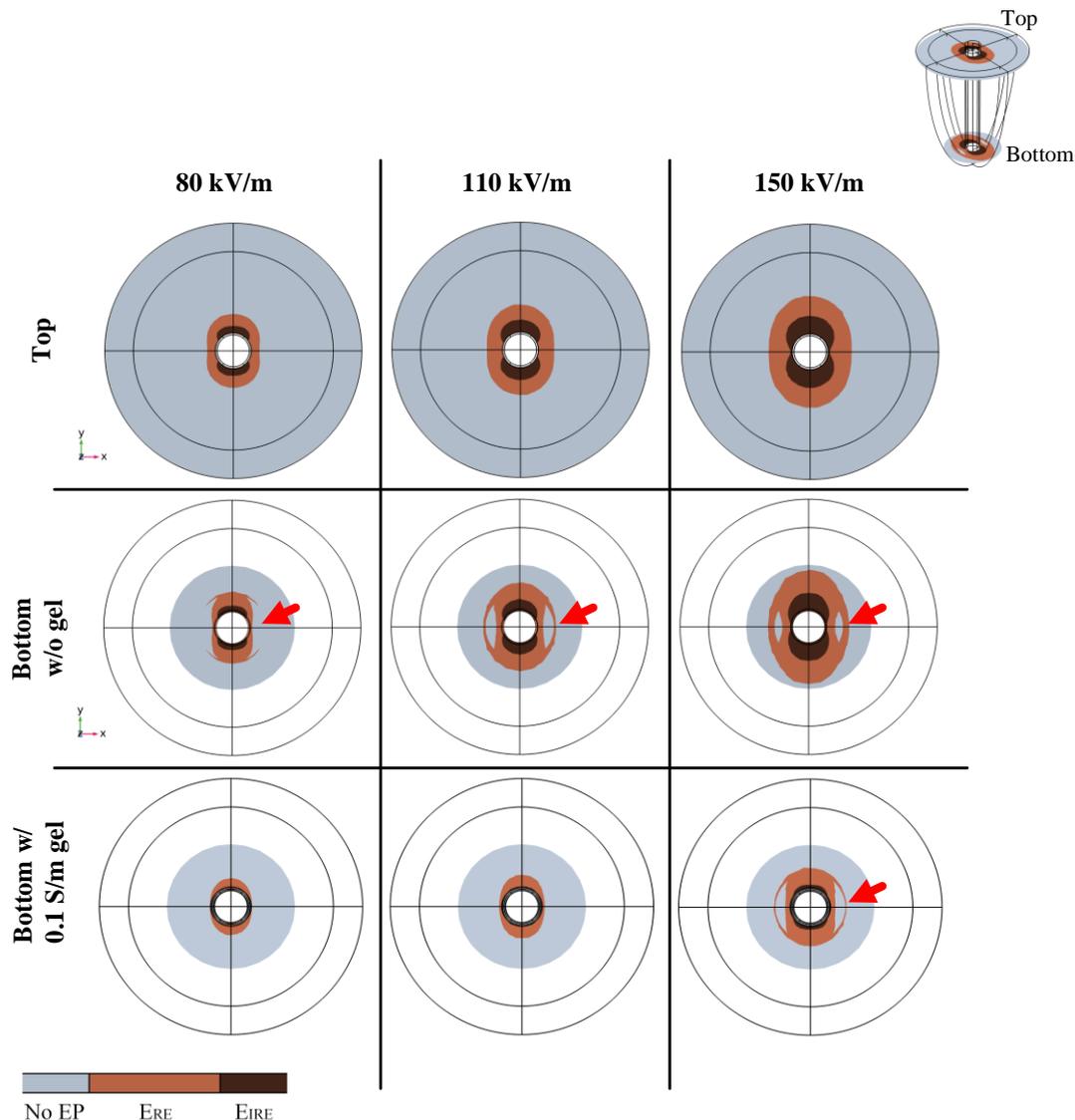| Electric Field (kV/m)	Electric current (A)	p (mm)
80	2.70	2.89
90	3.16	2.89
100	3.64	3.59
110	4.13	3.59
120	4.62	4.29
130	5.12	4.29
140	5.62	4.29
150	6.12	4.86

Figure 2. Slices show the top and bottom cut planes. Electric field distribution on top slices (where $p = 11.5$ mm) is less affected by the bone, whereas the bottom slices ($p = 1.89$ mm) are affected and show indentations (red arrows) for both without and with conductive gel. The bottom slices are the closest cut planes to the bone.

4. DISCUSSION

Currently, the ECT is applied in the treatment of clinical and veterinary cutaneous and subcutaneous tumors (Goanta and Ionita 2017, Probst *et al* 2018). For the treatment in complex body regions, it is recommended some pre-treatment studies. The pre-treatment can lead to personalized or improved electrode apparatus. Recent work shows that the ECT can also be successful in treating deep-seated nodules (Suzuki *et al* 2017, Simioni *et al* 2020, Falk Hansen *et al* 2020, Izzo *et al* 2020). Bone-neighboring neoplasms demand attention as the bone can change the EF distribution.

Table 1 and Fig. 2 showed that although higher electric fields cover larger tumor volumes, the indentation problem could not be avoided. Higher electric voltages translate to more significant volumes of indentation (with p from approximately 3 mm). Previous work has achieved similar results (Suzuki *et al* 2017). Indentation can be explained by the bone influence in the low-frequency electric field distribution. The tumor tissue is approximately 23 times more conductive than the bone; thus, bone behaves as an electrical insulator in the system, which affects the electric field distribution.

Computer simulations of biological models are interesting tools to study the nonlinear behavior of electrical conductivity in complex structures when exposed to electrical potentials (Miklavčič 2017). The electrical conductivity in tissues varies according to the type and geometric characteristics of the cells, the blood vascularization, the variation of

the hydrogen potential (pH) and the local oxygen concentration (Sieni *et al* 2020). In modeling process, it is often assumed that each geometry is completely homogeneous. In reality, however, the physiological structure of the body exhibits complex electrical properties. For example, the tumor is an anisotropic material consisting of different tissue arrangements. Moreover, it can be highly conductive depending on the site of growth and the degree of angiogenesis (Rosch and Markov 2004). Ideally, these properties should not be ignored when evaluating the electric field distribution. In this regard, although simulation models take into account the changes in electrical conductivity due to electroporation, to our knowledge there is not yet a model that estimates the electrical heterogeneity of tumors and their behavior due to the combination of these dynamics. Nevertheless, the homogeneous representation is still considered a solid approximation of tissue permeabilization while guarantee the safety standards for ECT. It also allows a rapid response in pre-treatment planning without the need for excessive animal testing.

Conductive gels are used in ECT procedures when an enhanced electrode-tissue contact in irregular areas is needed (Pintarelli *et al* 2019). However, in our tumor-bone case study, adding the conductive gel (Fig. 2) did not mitigate the electric field indentation. The gel is conductive and the bone dielectric; thus, causing the electrical currents to flow through the gel, decreasing the electric field propagation. Besides the opposite desired effect on ECT treatment, these results also draw attention to the possible overheating impact on the tissue due to high electric fields clustering in small extension areas.

With growing possibilities of cancer treatment using ECT, there is a need to optimized electrodes for most tumors. As the body has a natural sinuous characteristic, some tumor access could be challenging, thus, requiring a specific electrode design. Further research needs to be conducted to develop alternatives procedures to guarantee the total coverage in complex regions such as intranasal tumors. It is of our interest to investigate the electric field distribution in other newly developed electrodes based on volume coverage using animal realistic computational geometries and mimicking tissue phantoms (i.e. *in vitro* tests) to assess the electrical parameters.

5. CONCLUSION

In this work, we assessed the electric field distribution in a case study of a tumor in the intranasal region of a dog surrounded by bone tissue. We used computer simulations to evaluate the electrical parameters of the single-needle electrode recently developed to access and treat the area. We detect electric field disturbances caused by the low electrical conductivity of bone. We quantify the extent of the indentations, which starts at approximately 3 mm proximity of the electrode to the bone and increases with higher voltages. These electrical field disturbances can negatively affect treatment and ultimately lead to tumor recurrence. The application of conductive gel also narrows the field and reduces the electroporated volume compared to simulations without gel. Therefore, it is not recommended in this situation. By quantifying aspects of the application of the technique in such difficult areas, we alert electrochemotherapy practitioners for possible treatment failure. We also point out the need to improve methods of applying electroporation in bone-neigboring areas.

6. AKNOWLEGMENTS

7. REFERENCES

Falk Hansen H, Bourke M, Stigaard T, Clover J, Buckley M, O'Riordain M, Winter D C, Hjorth Johannesen H, Hansen R H, Heebøll H, Forde P, Jakobsen H L, Larsen O, Rosenberg J, Soden D and Gehl J 2020 Electrochemotherapy for colorectal cancer using endoscopic electroporation: a phase 1 clinical study *Endosc. Int. Open* **08** E124–32
Gabriel C, Gabriel S and Corthout E 2000 The dielectric properties of biological tissues: III. Parametric models for the dielectric spectrum of tissues *Phys. Med. Biol.* **41** 2271–94 Online: http://iopscience.iop.org/article/10.1088/0031-9155/41/11/003/pdf
Gehl J, Sersa G, Matthiessen L W, Muir T, Soden D, Occhini A, Quaglino P, Curatolo P, Campana L G, Kunte C, Clover A J P, Bertino G, Farricha V, Odili J, Dahlstrom K, Benazzo M and Mir L M 2018 Updated standard operating procedures for electrochemotherapy of cutaneous tumours and skin metastases *Acta Oncol. (Madr).* **57** 874–82 Online: https://doi.org/10.1080/0284186X.2018.1454602
Goanta A M and Ionita L 2017 Electrochemotherapy: a Review of Its Use and Limitations in Small Animal Oncology *Agrolife Sci. J.* **6** 125–32
Heinz V, Alvarez I, Angersbach A and Knorr D 2001 Preservation of liquid foods by high intensity pulsed electric fields - Basic concepts for process design *Trends Food Sci. Technol.* **12** 103–11
Izzo F, Ionna F, Granata V, Albino V, Patrone R, Longo F, Guida A, Delrio P, Rega D, Scala D, Pezzuto R, Fusco R, Di Bernardo E, D'Alessio V, Grassi R, Contartese D and Palaia R 2020 New deployable expandable electrodes in

the electroporation treatment in a pig model: A feasibility and usability preliminary study *Cancers (Basel).* **12**

Kluthcovsky L C, Queiroz T N de L, Somensi M, Castro J L C and Engracia Filho J R 2021 Angiofibroma of the Nasal Cavity in a Dog: Case Report *Top. Companion Anim. Med.* **44**

Kotnik T, Frey W, Sack M, Haberl Meglič S, Peterka M and Miklavčič D 2015 Electroporation-based applications in biotechnology *Trends Biotechnol.* **33** 480–8

Maglietti F, Tellado M, Olaiz N, Michinski S and Marshall G 2017 Minimally invasive electrochemotherapy procedure for treating nasal duct tumors in dogs using a single needle electrode *Radiol. Oncol.* **51** 422–30

Miklavčič D 2017 *Handbook of Electroporation* vol 1–4

Mir L M, Gehl J, Sersa G, Collins C G, Garbay J R, Billard V, Geertsen P F, Rudolf Z, O'Sullivan G C and Marty M 2006 Standard operating procedures of the electrochemotherapy: Instructions for the use of bleomycin or cisplatin administered either systemically or locally and electric pulses delivered by the CliniporatorTM by means of invasive or non-invasive electrodes *Eur. J. Cancer, Suppl.* **4** 14–25

Pintarelli G B, Berkenbrock J A, Rassele A, Rangel M M M and Suzuki D O H 2019 Computer simulation of commercial conductive gels and their application to increase the safety of electrochemotherapy treatment *Med. Eng. Phys.* **74** 99–105 Online: https://doi.org/10.1016/j.medengphy.2019.09.016

Prausnitz M R, Bose V G, Langer R and Weaver J C 1993 Electroporation of mammalian skin: A mechanism to enhance transdermal drug delivery *Proc. Natl. Acad. Sci. U. S. A.* **90** 10504–8

Probst U, Fuhrmann I, Beyer L and Wiggermann P 2018 Electrochemotherapy as a new modality in interventional oncology: A review *Technol. Cancer Res. Treat.* **17** 1–12

Rosch P J and Markov marko S 2004 *Bioelectromagnetic Medicine*

Rubinsky B 2007 Irreversible electroporation in medicine *Technol. Cancer Res. Treat.* **6** 255–9

Šel D, Cukjati D, Batiuskaite D, Slivnik T, Mir L M and Miklavčič D 2005 Sequential finite element model of tissue electropermeabilization *IEEE Trans. Biomed. Eng.* **52** 816–27

Sieni E, Sgarbossa P, Mognaschi M E, Forzan M, Parupudi T, Mittal L, Camarillo I G and Sundararajan R 2020 Electric field distribution study in inhomogeneous biological tissues *Int. J. Numer. Model. Electron. Networks, Devices Fields* **33** 1–13

Simioni A, Valpione S, Granziera E, Rossi C R, Cavallin F, Spina R, Sieni E, Aliberti C, Stramare R and Campana L G 2020 Ablation of soft tissue tumours by long needle variable electrode-geometry electrochemotherapy: final report from a single-arm, single-centre phase-2 study *Sci. Rep.* **10** 1–13 Online: http://dx.doi.org/10.1038/s41598-020-59230-w

Suzuki D O H, Berkenbrock J A, Frederico M J S, Silva F R M B and Rangel M M M 2018 Oral Mucosa Model for Electrochemotherapy Treatment of Dog Mouth Cancer: Ex Vivo, In Silico, and In Vivo Experiments *Artif. Organs* **42** 297–304

Suzuki D O H, Berkenbrock J A, de Oliveira K D, Freytag J O and Rangel M M M 2017 Novel application for electrochemotherapy: Immersion of nasal cavity in dog *Artif. Organs* **41** 767–73

Suzuki D O H, Ramos A, Ribeiro M C M, Cazarolli L H, Silva R M B, Leite L D and Marques J L B 2011 <Electroporated Membran Conductance Theory and Experiment 2011.pdf> **58** 3310–8

Tamzali Y, Borde L, Rols M P, Golzio M, Lyazrhi F and Teissie J 2012 Successful treatment of equine sarcoids with cisplatin electrochemotherapy: A retrospective study of 48 cases *Equine Vet. J.* **44** 214–20

Teissié J and Rols M P 1993 An experimental evaluation of the critical potential difference inducing cell membrane electropermeabilization *Biophys. J.* **65** 409–13

8. RESPONSIBILITY NOTICE

The authors are the only responsible for the printed material included in this paper.